ADVANCE COPY: This paper has been submitted for publication in the ASME Journal of Dynamic Systems, Measurement and Control. It will also be presented at the ASME 1985 Winter Annual Meeting.

THE IDENTIFICATION OF THE QUADRATIC SYSTEM RELATING CROSS-FLOW AND IN-LINE, VORTEX-INDUCED VIBRATION

by

Jen-Yi Jong, Wyle Laboratories

J. Kim Vandiver, Massachusetts Institute of Technology

ABSTRACT

This paper presents an application of the multiple regression method to the identification of the nonlinear relationship between cross-flow and in-line, vortex-induced vibration. Previous results of bispectral analysis of the Castine data by Jong [7] indicated that cross-flow and in-line response are correlated quadratically for both lock-in and non-lock-in cases. Therefore, a second order nonlinear system was used to model the relationship between cross-flow and in-line vibration. The cross-flow response is treated as the input to the nonlinear system and the in-line response is defined as the output. Both time domain and frequency domain multiple regression methods are presented in the evaluation of the quadratic system function under lock-in and non-lock-in conditions respectively. Nonlinear input/output correlations higher than second order in the relationship are shown to be negligble.

NOMENCLATURE

$x(t)$	cross-flow acceleration
$y(t)$	in-line acceleration
$y_1(t)$	output from the Case 1 square law operator
$y_2(t)$	output from the Case 2 square law operator
$y_s(t)$	simulated in-line response
y_o	d.c. component of the in-line response
$n(t)$	noise
$g(u,v), g_1(\ ), g_2(\ )$	second order impulse response function
$h(u)$	linear impulse response function
$G(w)$	special form of $g(u,v)$
K	order of linear convolution
M	order of the second order convolution
$G(W_1,W_2), G_1(W_1,W_2) G_2(W_1,W_2)$	Fourier transforms of g, g_1, and g_2
$H(w), H_1(W), H_2(W)$	Fourier transform of $h(u)$, $h_1(w)h_2(u)$
MSE	mean square error
$E[\ ]$	expected value operator
$Sxx(W)$	auto spectrum of x(t)
$Sxy(W)$	cross spectrum of x(t) and y(t)
$Bxxx(Wp,Wq)$	auto bispectrum of x(t)
$Bxxy(Wm,Wn)$	cross bispectrum of y(t) and x(t)
W	frequency (radians/sec)
$\delta(\ )$	delta function
$\underline{I}$	unity vector
	underscore indicates a vector
$\overline{[\ ]}$	square brackets indicate a matrix

INTRODUCTION

Marine risers, pipelines, and hydrophone cables are all examples of structures subjected to vortex-induced vibration. The response of the cylinder depends on a complex interaction between the natural modes of the vibration and the vortex-shedding process. The implementation of good design procedures that account for strumming vibration is becoming more essential as the offshore industry moves into deeper water.

In a spatially uniform flow, lock-in may occur when the vortex-shedding frequency is within a few percent of a cylinder's natural frequency. Sustained periodic vibration results in both in-line and cross-flow directions. The cross-flow motion is dominated by one mode at the natural frequency of the cylinder. The in-line motion is dominated by a frequency twice that of the cross-flow motion. Typical in-line amplitudes are one-half that of the cross-flow displacement [8].

When the shedding frequency is outside the lock-in bandwidth, non-lock-in occurs and the response time histories in both in-line and cross-flow directions are best described as random processes. Several modes may respond in both directions. The cross-flow response frequencies are generally dominated by natural frequencies of the cylinders. The response frequencies typical of the in-line motion are not typically natural frequencies, but are most closely associated with sums of frequencies of dominant cross flow spectral peaks. The evidence of frequency doubling and summing under lock-in and non-lock-in conditions supports the hypothesis that in-line and cross-flow response are non-linearly correlated. As an initial test a bispectral analysis of flow induced vibration data obtained during a field test at Castine, Maine, was performed by Jong [7]. A very clear nonlinear correlation was evident between in-line and cross-flow vibration. The cross-bicoherence provided conclusive evidence that cross-flow and in-line response are correlated

quadratically for both lock-in and non-lock-in cases. These conclusions suggested that, in general, a second order nonlinear system can be used to model the relationship between cross-flow and in-line response.

The data analyzed in this paper was gathered during a field test in Castine, Maine in 1981. The experimental arrangements are described in Refs. 7 and 17 and are very briefly described here. A steel tube 75 feet of the long (22.86 m) and 1.625 inches in diameter (4.13 cm) was suspended horizontally under tension between two pilings. A spatially uniform tidal current normal to the longitudinal axis of the cylinder provided the vortex related excitation. Tension, current, drag force, and seven biaxial cylinder accelerations were recorded. Reynolds numbers of 300 to 20,000 were encountered.

The purpose of the research described in this paper was to examine the adequacy of a second order system in modelling flow induced vibration as observed in the Castine tests and to show that significant contributions, due to higher order nonlinearities, do not exist. To address this issue a quadratic system identification was performed for both the previous lock-in and non-lock-in cases. Due to the nature of nearly deterministic lock-in response, a time domain, multiple regression method was applied in the system identification procedure, while a frequency domain error minimization method was used for the non-lock-in, random vibration cases. The results showed that nonlinearities higher than second order were negligible for both lock-in and non-lock-in. Linear and second order correlation exist at lock-in. Whereas, in-line and cross-flow responses were linearly independent at non-lock-in and quadratic correlation accounted for all but a small amount of the nonlinear correlation between in-line and cross-flow vibration.

QUADRATIC SYSTEM IDENTIFICATION AT LOCK-IN

Initially, the bispectrum analysis was used to identify the quadratic correlation between cross-flow and in-line vibration. In this section, the relationship between cross-flow and in-line response is modelled with a second order nonlinear system, including a linear term and quadratic term. An error term is also introduced to represent imperfections of the model which might be due to the existence of the higher order nonlinearities. The linear and quadratic impulse response functions are identified for the lock-in case by using a time domain multiple regression method. By one and two dimensional convolution of the identified linear and quadratic impulse response functions with the measured cross-flow response, the in-line response can be predicted. The predicted and measured in-line response agree very well, as will be demonstrated with Castine field test data.

Application of Multiple Regression Analysis

Let the input x(t) be the cross-flow response, and output y(t), the in-line response. x(t) and y(t) are assumed to be related by a second order system as follows.

$$y(t) = yo + \sum_{u=0}^{k-1} h(u)x(t-u) + \sum_{u=0}^{M-1}\sum_{v=0}^{M-1} g(u,v)x(t-u)x(t-v)+n(t) \qquad (1)$$

where n(t) is the error term, h(u) is the linear impulse response function and g(u,v) is the second order impulse response kernel. Given the measured input and output data, x(t) and y(t)=1,2,...(N+K-1). the system functions h(u) and g(u,v) are to be determined in such a way that the estimated mean square error (MSE) is minimized. It was assumed with no loss of generality, that the second order impulse response kernel is symmetrical in its arguments:

$$g(u,v)=g(v,u) \qquad (2a)$$

and thus their Fourier transforms are also symmetrical

$$G(W_1,W_2)=G(W_2,W_1) \qquad (2b)$$

Consequently, the quadratic transfer function is symmetric about the line $W_1=W_2$ in the bi-frequency plane. Equation (1) can then be rewritten in matrix form as:

$$\underline{y}=\underline{yo}+[x]\underline{h}+[z]\underline{G}+\underline{n} \qquad (3)$$

where

unknowns h(u) u=0,1,...,K-1

unknowns g(u,v) u=0,1,...,M-1 v=0,1,...,M-1

NN=N+K-1 , MM=M(M+1)/2

z(t,w)=x(t-u)x(t-v) with

w=v+M*u-u(u+1)/2

$$G(w)=\begin{cases} g(u,v) & \text{if } u=v \\ 2g(u,v) & \text{if } u=v \end{cases}$$

$\underline{h}=[\ h(0),h(1),.....h(K-1)]^T$ Kx1 vector

$\underline{y}=[y(K),y(K+1),.....y(NN)\ ]^T$ Nx1 vector

$\underline{n}=[\ n(K),n(K+1),.....n(NN)\ ]^T$ Nx1 vector

$\underline{yo}=[\ yo,yo,.....y_o\ \ ]^T$ Nx1 vector

$\underline{G}=[G(0),G(1),.....G(MM-1)\ ]^T$ MMx1 vector

$$[x]=\begin{bmatrix} x(K) & x(K-1) & x(K-2).....x(1) \\ x(K+1) & x(K+2) & x(K+3).....x(2) \\ \vdots & & \\ x(N+K-1) & x(N+K-2) & .....x(N) \end{bmatrix}$$

NxK matrix

$$[z]=\begin{bmatrix} z(K,0) & z(K,1).....z(K,MM-1) \\ z(K+1,0) & z(K+1,1)....z(K+1,MM-1) \\ \vdots & \\ z(K+N-1,0) & z(K+N-1,1)..z(K+N-1,MM-1) \end{bmatrix}$$

NxMM matrix

the MSE can be written as

$$MSE=\underline{n}^T[\underline{n}] =$$

$$(\underline{y}-\underline{yo}-\underline{h}[x]-\underline{G}[z])(\underline{y}-\underline{yo}-[x]\underline{h}-[z]\underline{G})=$$

$$\underline{y}^T\underline{y}-2\underline{h}^T[x]^T\underline{y}-2\underline{G}^T[z]^T\underline{y}+$$

$$2\underline{h}^T[x]^T[z]\underline{G}+\underline{h}^T[x]^T[x]\underline{h}+$$

$$\underline{G}^T[z]^T[z]\underline{G}-\underline{yo}^T(\underline{y}-[x]\underline{h}-[z]\underline{G})-$$

$$(\underline{y}^T-\underline{h}^T[x]^T-\underline{G}^T[z]^T)\underline{yo}+$$

$$\underline{yo})^T\underline{yo} \qquad (4)$$

Seeking minima in the MSE with respect to yo, hi, and Gi leads to:

let $\partial MSE/\partial\ yo=0$, resulting in

$$N*yo+\underline{I}^T[x]\underline{h}+\underline{I}^T[z]\underline{G}=\underline{I}^T\underline{y} \qquad (5)$$

let $\partial MSE/\partial\ hi=0$, resulting in

$$([x]^T[z]\underline{G}+([x]^T[x])\underline{h}+yo[x]^T\underline{I}=[x]^T\underline{y} \qquad (6)$$

let $\partial\ MSE/\partial\ Gi=0$, resulting in

$$([z]^T[x])\underline{h}+([z]^T[z])\underline{G}+yo[z]^T\underline{I}\ =[z]^T\underline{y} \qquad (7)$$

These three equations can be combined and rewritten as

$$\begin{bmatrix} [M1] & [C] & \underline{Q1}^T \\ [C]^T & [M2] & \underline{Q2}^T \\ \underline{Q1} & \underline{Q2} & N \end{bmatrix} \begin{Bmatrix} \underline{h} \\ \underline{G} \\ yo \end{Bmatrix} = \begin{Bmatrix} \underline{R1} \\ \underline{R2} \\ Ro \end{Bmatrix} \qquad (8)$$

where

$Ro=\underline{I}^T\underline{y}$ = constant

$\underline{R1}=[x]\underline{y}$=Kx1 vector

$\underline{R2}=[z]\underline{y}$=MMx1 vector

$\underline{Q1}=\underline{I}[x]$=1xK vector

$\underline{Q2}=\underline{I}[z]$=1xMM vector

[M1]=[x][x]=KxK matrix

[M2]=[z][z]=MMxMM matrix

[C]=[x][z]=KxMM matrix

For a specified order K and M, the system functions h(u) and g(u,v) can be obtrained by solving the set of linear equations (8) with x(t) and y(t) being the cross-flow and in-line responses respectively. The identified system functions h(u) and g(u,v), can be convolved with the measured cross-flow response x(t) to produce predicted linear and quadratic components of the in-line response y1(t) and y2(t) respectively as shown in equation (9). The total predicted in-line response ys(t) and the residual noise terms are also given.

a. $n(t) = y(t)-ys(t)$

b. $ys(t) = y_o+y_1(t) + y_2(t)$

c. $$y_1(t) = \sum_{u=0}^{K-1} h(u)x(t-u) \qquad (9)$$

d. $$y_2(t) = \sum_{u=0}^{M-1}\sum_{v=0}^{M-1} g(u,v)x(t-u)x(t-v)+y_o$$

AN EXAMPLE FOR THE LOCK-IN CASE

In this section, results are presented in which typical lock-in response data were analyzed by using the time domain multiple regression method described in the previous section. The data was obtained from a vibrating, horizontal steel tube 75 feet in length and 1.625 inches in diameter. The tube behaved dynamically as a uniform beam under tension with pinned ends. The mode shapes in both cross-flow (vertical plane) and in-line (horizontal plane) directions were sine waves. The natural frequencies were unequally spaced due to the bending stiffness of the beam. The natural frequencies are the same in the cross-flow and in-line directions. Vortex shedding excited at various times from the second to the tenth modes of vibration. At any given time, the cross-flow and in-line vibration occured in different modes and at different frequencies.

The tube contained seven biaxial pairs of accelerometers distributed along the axis of the tube. The accelerometers measured in-line and cross-flow vibration. Figure 1 shows a time history of motion in the x-y plane measured by a pair of accelerometers located at one fourth of the length of the tube from one end. The figure eight pattern is the result of lock-in cross-flow vibration in the third mode and in-line vibration in the fifth mode. The fifth mode natural frequency is twice the natural frequency of the third mode. The one fourth point of the span is near an anti-node for both mode shapes. At L/4 both node shapes have 70.7% of their maximum anti-node value. The vortex shedding process under lock-in conditions generates a periodic zero mean lift force distributed coherently along the span of the tube. The vortex shedding also creates a non-zero mean drag force which has fluctuating component at twice the frequency of the lift force.

In this example the drag force excitation frequency coincided with the fifth natural frequency of the tube in the in-line direction. The figure eight pattern indicates that although the in-line and cross-flow motions are at different frequencies, they are highly correlated. These x(t) and y(t) measured time series were used in equation (8) to calculate the system functions h(t) and g(u,v) from which the error n(t) was then obtained. By increasing the order K and M, a convergent MSE was reached. The error n(t) for K=30 and M=9 was a wide-band noise indicated by its flat spectrum. The ratio between the MSE and the variance of in-line response was 2.6%. This small amount of wide-band error implied that nonlinearities higher than second order were negligible for the lock-in case and the second order nonlinear system was a reasonable model, relating the cross-flow and in-line response.

From equation (9b), a simulated in-line response ys(t) was obtained which was in good agreement with the measured in-line response y(t). This agreement is easier to visualize by comparing the x-y diagram of cross-flow response x(t) vs. simulated in-line response ys(t), as shown in Figure 2 to the measured x versus y data shown in Figure 1. The linear and quadratic components of the predicted in-line response $y_1(t)$ and $y_2(t)$ were calculated from equations (9c and 9d). The x-y diagrams of x(t) vs. $y_1(t)$ and x(t) vs. $y_2(t)$ in Figure 3 and 4 show that the linear in-line response and quadratic in-line response contribute quite different patterns to the total in-line

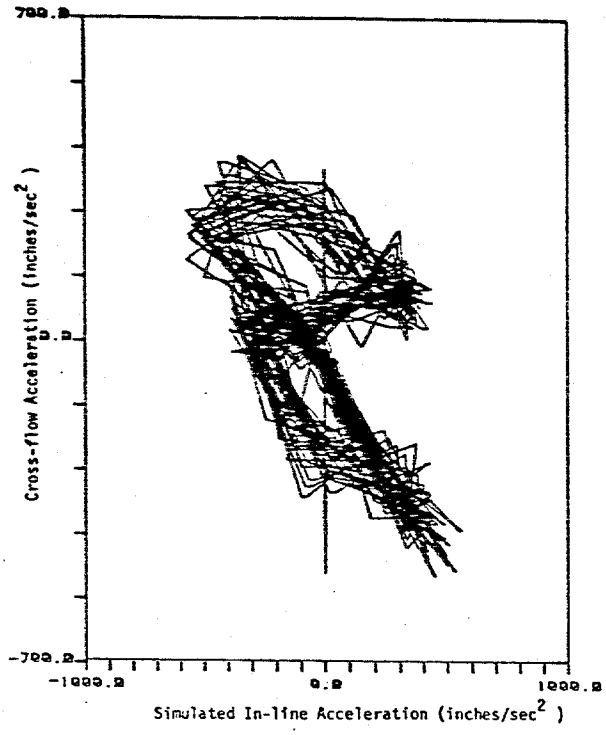

FIG. 1. X, Y Diagram of In-Line Versus Cross-Flow Acceleration

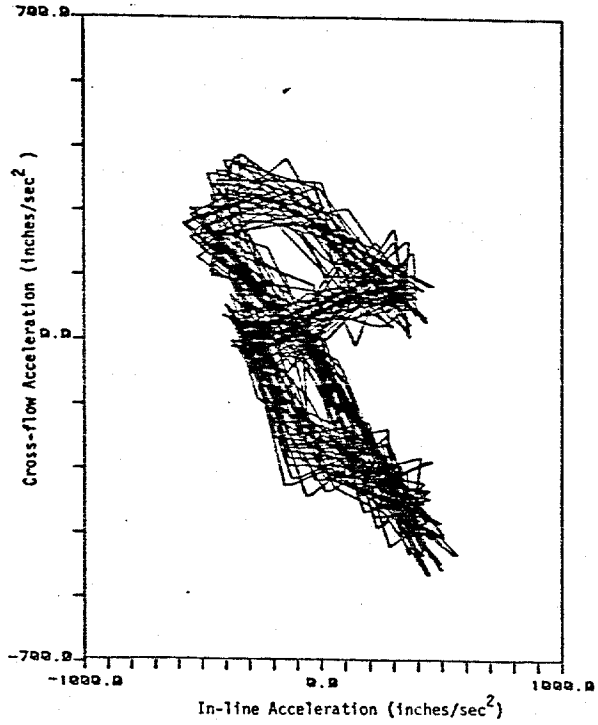

FIG. 2. X, Y Diagram of Cross-Flow Versus Simulated In-Line Acceleration

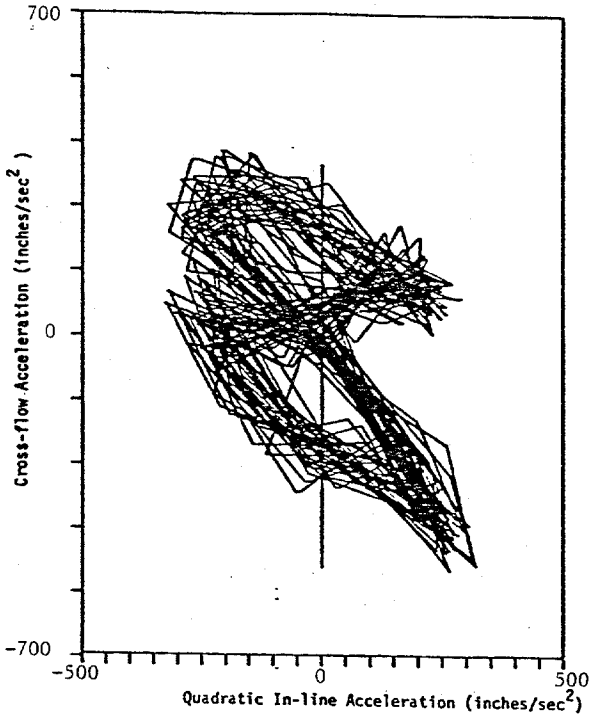

FIG. 3. X, Y Diagram of Cross-Flow Versus The Quadratic Component of In-Line Acceleration

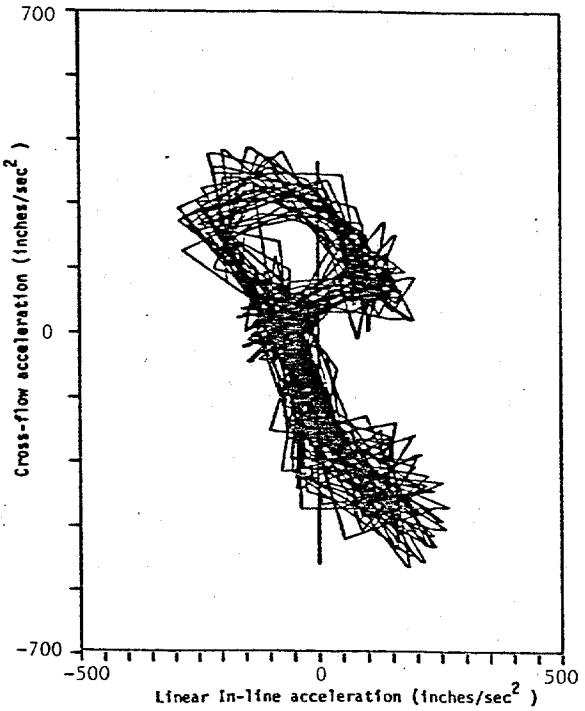

FIG. 4. X, Y Diagram of Cross-Flow Versus The Linear Component of In-Line Acceleration

response.

When the multiple regression method was applied to the non-lock-in case, the rate of convergence was much slower than that of the lock-in case and became inefficient due to the required larger order of K and M. The reason for the slower convergence is that at lock-in, the response time series are quite deterministic. Therefore, only a little past information is required to predict the present response, while the responses at non-lock-in are much more random than the lock-in responses leading to the requirement of a higher order of K and M in equation (1). The quadratic system identification for the non-lock-in case will be discussed in the next section.

QUADRATIC SYSTEM IDENTIFICATION AT NON-LOCK-IN

In this section, a frequency domain multiple regression method for quadratic system identification will be discussed for the non-lock-in case. A quadratic model involving a square law system proposed by Bendat and Piersol [3] is used in the system identification. The residual error is used to evaluate the existance of higher order nonlinearities in the system input/output relationship. High linear coherence between the in-line response and the square of cross-flow response is demonstrated, which provides additional evidence of the existence of quadratic correlation between in-line and cross-flow response.

Least Squares Quadratic System Identification

A frequency domain quadratic system identification method with the input, a stationary Gaussian random process has been used by several other researchers [5,11]. The method is applied here to non-lock-in response data to obtain the quadratic transfer function.

The input and output of a quadratic system is expressed as given in Equation 1:

$$y(t)=\sum h(u)x(t-u)+\sum\sum g(u,v)x(t-u)x(t-v)+n(t) \qquad (1)$$

where n(t) denotes any error associated with the imperfection of the model or noise in the system. Here, a linear term is included even though the in-line and cross-flow response are almost linearly independent [7] for the non-lock-in case. The transfer functions H(W) and $G(W_1, W_2)$, are to be determined such that the mean square error, MSE, of n(t) is minimized. The MSE can be expressed as,

$$MSE=E[n^2(t)]=E[y(t)-\sum h(u)x(t-u)-\sum\sum g(u,v)x(t-u)x(t-v)]^2 \qquad (10)$$

Let
$[x(t),X(W)],[y(t),Y(W)],[h(u),H(W)],[g(u,v),G(W_1,W_2)]$

be Fourier transform pairs. We find that

$$MSE=E\Big[\sum_{j=-K}^{K}(Y(Wj)-H(Wj)X(Wj)-\sum_{p+q=j}\sum G(Wp,Wq)X(Wp)X(Wq)\exp(iWjt)\Big]^2$$

$$=\sum_{j=-K}^{K}E[Y(Wi)-H(Wj)X(Wj)-\sum_{p+q=j}\sum G(Wp,Wq)X(Wp)X(Wq)]^2 \qquad (11)$$

$$=\sum_{j=-K}^{K}E[Y(Wj)]^2+[H(Wj)]^2-H(Wj)X(Wj)Y^*(Wj)-H^*(Wj)X^*(Wj)Y(Wj)$$
$$-\sum_{p+q=j}\sum G(Wp,Wq)Y^*(Wj)X(Wp)X(Wq)+\sum_{p+q=j}\sum H^*(Wj)G(Wp,Wq)X^*(Wj)X(Wp)X(Wq)-\sum_{p+q=j}\sum G^*(Wp,Wq)Y(Wj)X^*(Wp)X^*(Wq)+\sum_{p+q=j}\sum (Wj)G^*(Wp,Wq)X(Wj)X^*(Wp)X^*(Wq)+\sum_{p+q=j}\sum G(Wp,Wq)G^*(Wr,Ws)X(Wp)X(Wq)X^*(Wr)X^*(Ws) \qquad (12)$$

Let $\partial MSE/\partial H(Wj)=0$, and $\partial MSE/\partial G(Wm,Wn)=0$ with $Wm+Wn=Wj$ for all Wj. We obtain

$$H^*(Wj)E[X(Wj)^2]=E[X(Wj)Y^*(Wj)]+\sum_{p+q=j}\sum G^*(Wp,Wq)E[X(Wj)X^*(Wp)X^*(Wq)] \qquad (13)$$

$$E[Y^*(Wj)X(Wm)X(Wn)]=H^*(Wj)E[X^*(Wj))X(Wm)X(Wn)]+\sum_{p+q=j}\sum G^*(Wp,Wq)E[X^*(Wp)X^*(Wm)X(Wn)] \qquad (14)$$

From the following definitions,

$$Sxx(Wj)=E[X(Wj)X(-Wj)]$$

$$Sxy(Wj)=E[X(Wj)Y(-Wj)] \qquad (15)$$

$$Bxxx(Wp,Wq)=E[X(Wp)X(Wq)X(-Wp-Wq)]$$

$$Bxxy(Wm,Wn)=E[X(Wm)X(Wn)Y(-Wm-Wn)]$$

Equations (13) and (14) can be rewritten as:

$$H^*(Wj)Sxx(Wj)=Syx(Wj)+\sum_{p+q=j}\sum G^*(Wp,Wq)Bxxx(Wp,Wq) \qquad (16)$$

$$Bxxy(Wm,Wn)=H^*(Wj)Bxxx(Wm,Wn)+\sum_{p+q=j}\sum G^*(Wp,Wq)E[X^*(Wp)X^*(Wq)X(Wm)X(Wn)] \qquad (17)$$

From these two equations, we see that the determination of the transfer functions H(W) and $G(W_1,W_2)$ required the estimation of the fourth order spectrum, which is difficult, due to computer storage limitations. However, if the input x(t) is a Gaussian random process, this problem can be simplified considerably. If x(t) is a Gaussian random process, the bispectrum Bxxx(Wm,Wn) is zero, and we can write the fourth order cumulant spectrum as:

$$E[X^*(Wp)X^*(Wq)X(Wm)X(Wn)]=E[X^*(Wp)X^*(Wq)]E[X(Wm)X(Wn)]+E[X^*(Wp)X(Wm)]E[X^*(Wq)X(Wn)]+E[X^*(Wp)X(Wn)]E[X^*(Wq)X(Wm)]=$$
$$\delta(Wp+Wq)\,\delta(Wn+Wm)Sxx(Wp)Sxx(Wm)+\delta(Wp-Wm)\,\delta(Wq-Wn)Sxx(Wm)Sxx(Wn)+\delta(Wp-Wn)\,\delta(Wq-Wm)Sxx(Wm)Sxx(Wn) \qquad (18)$$

The last term in equation (17) for nonzero Wj becomes

$$\Sigma\Sigma G(Wp,Wq)E[X^*(Wp)X^*(Wq)X(Wm)X(Wn] = \underset{p+q=j}{} 2G(Wm,Wn)Sxx(Wm)Sxx(Wn) \quad (19)$$

Finally we obtain

$$H(W) = Sxy(W)/Sxx(W) \quad (20)$$

$$G(W_1,W_2)=B^*xxy(W_1,W_2)/2Sxx(W_1)Sxy(W_2) \quad (21)$$

These two equations can be used to determine the linear and quadratic transfer functions, and only require the estimation of the spectra Sxx(W), Sxy(W), and the cross-bispectrum $Bxxy(W_1,W_2)$ for a Gaussian input. It has been shown [7] that the non-lock-in cross-flow response can be approximated by a Gaussian random process as deduced from the Chi-square goodness-of-fit test on the response histogram of the Castine data.

Figures 6 and 5 show the power spectra of the cross-flow and in-line response at non-lock-in. The cross-bicoherence spectrum between these two responses, as shown in Figure 7, indicates a significant quadratic correlation between them. Figure 8 shows the magnitude of the quadratic transfer function $G(W_1,W_2)$ at non-lock-in based on equation (21) with the input cross-flow response a Gaussian random process. Note that in this figure of $G(W_1,W_2)$, all the peaks tend to be concentrated along the 45 degree lines in the bi-frequency plane. While $G(W_1,W_2)$ is the two-dimensional Fourier transform of the second order impulse response kernel g(u,v), for a general quadratic system, it need not possess this particular property. This observation implies that this quadratic system has certain properties which might enable further simplification of the system in the non-lock-in case. A special quadratic system possessing this particular property has been formulated by Bendat and Piersol and will be discussed in the next section.

QUADRATIC SYSTEMS INVOLVING SQUARE-LAW OPERATORS

Two models of a quadratic system which involve a zero memory square-law system, as pictured in Figure 9, have been analyzed by Bendat and Piersol and are briefly discussed here. The zero memory square law system is either followed or preceded by a constant parameter linear system. The properties of these two models, referred to as Case 1 and Case 2, were examined to check if either of them could be used to simplify the quadratic system identification problem for the non-lock-in case.

The combinations of a square-law system and a linear system give the relations between x(t) and y1(t), y2(t) as, from Case 1

$$y1(t)=h1(t)*[x(t)]^2$$

$$= \int h_1(u)[x(t-u)]^2du$$

$$= \int\int h_1(u)\delta(u-v)x(t-u)x(t-v)du\ dv$$

$$= \int\int g_1(u,v)x(t-u)x(t-v)du\ dv \quad (22)$$

from Case 2

$$y2(t)=[h_2(t)*x(t)]^2$$

$$= [\int h_2(u)x(t-u)du]^2$$

$$= \int\int h_2(u)h_2(v)x(t-u)x(t-v)du\ dv$$

$$\int\int g_2(u,v)x(t-u)x(t-v)\ du\ dv \quad (23)$$

where * denotes the linear convolution and $\delta(u)$ is the delta function. The second order impulse response kernals for these two cases are

$$g_1(u,v)=h_1(u)\delta(u-v) \quad (24)$$

$$g_2(u,v)=h2(u)h_2(v) \quad (25)$$

The Fourier transforms of these two equations give the quadratic transfer functions $G_1(W_1,W_2)$ and $G_2(W_1$ as,

$$G_1(W_1,W_2)=H_1(W_1+W_2) \quad (26)$$

$$G_2(W_1,W_2)=H_2(W_1)H_2(W_2) \quad (27)$$

The system function $H_1(W)$ and $H_2(W)$ can be obtained by writing equations (26) and (27) as

$$G_1(W/2,W/2)=H_1(W/2+W/2)=H_1(W) \quad (28)$$

$$G_2(W,W)=H_2^2(W) \quad (29)$$

By using equation (21) for quadratic system identification with Gaussian inputs, we obtain

$$H_1(W)=G_1(W/2,W/2) = Bxxy_1(W2,W/2)/2S^2xx(W/2) = Bxy_1(W/2)/2S^2xx(W/2) \quad (30)$$

$$H_2(W)=SQRT[G_2(W,W)]=Bxxy^2(W,W)/2S^2xx(w) = Bxy^2(w)/2S^2xx(W) \quad (31)$$

In which Bxy(W) is the special bispectral density function defined by

$$Bxy(W)=Bxxy(W,W)=E[X(W)X(W)Y(2W)] \quad (32)$$

Equations (30) and (31) were derived from the least square error point of view and they are identical to the results formulated by Bendat.

The linear transfer function H(W) derived by Bendat is also identical to the results of section 4 which was

$$H(W)=Sxy(W)/Sxx(W) \quad (33)$$

Checking the properties of the quadratic transfer functions in equations (26) and (27) permits one to determine whether or not the Case 1 model or the Case 2 model is more appropriate to fit to the non-lock-in data. According to equation (26) for Case 1, any peak associated with the function $H_1(W)$ will show up along a 45-degree line in the bi-frequency plane of $G_1(W_1,W_2)$ which is similar to the result stated in section 4, while Case 2 does not possess this property. The Case 1 model was chosen to model the non-lock-in response data. The goodness of fit of the Case 1 model would be checked by the residual n(t).

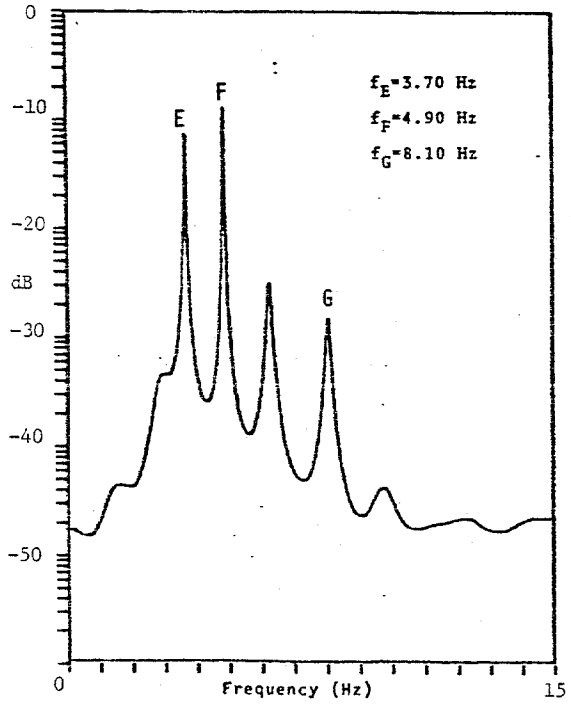

FIG. 5. Power Spectrum of In-Line Acceleration at Non-Lockin

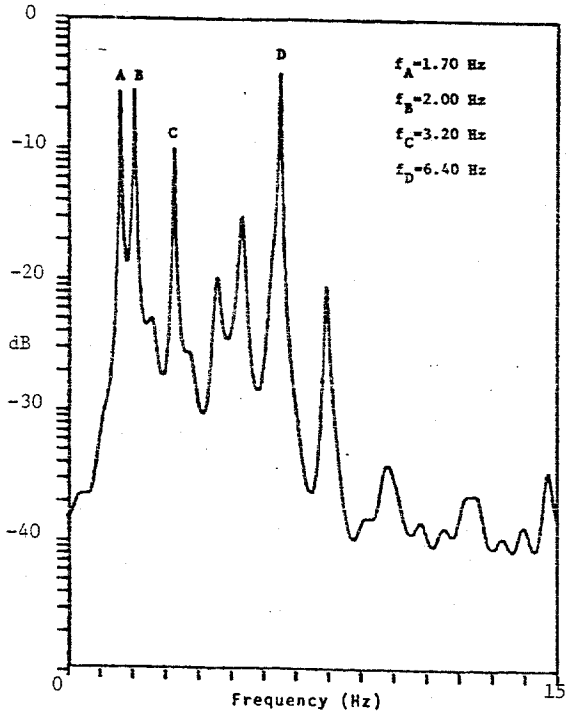

FIG. 6. Power Spectrum of Cross-Flow Acceleration at Non-Lockin

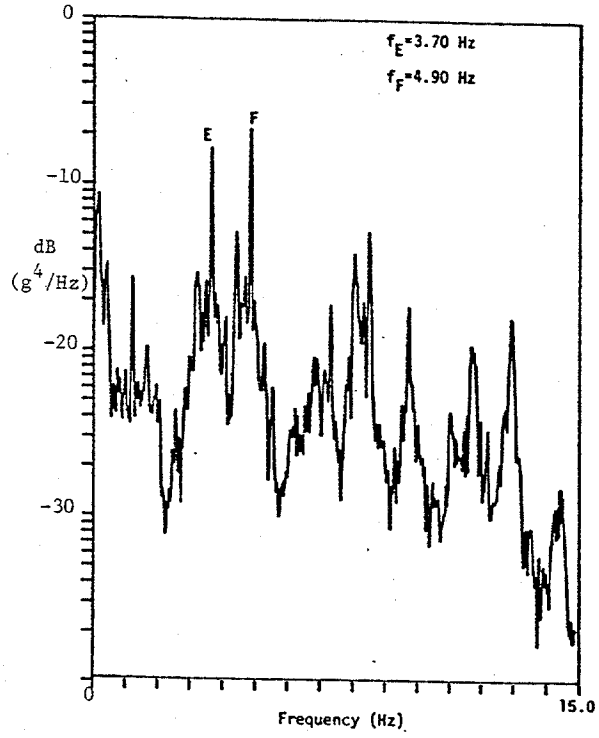

FIG. 10. Power Spectrum of the Square of the Cross-Flow Acceleration

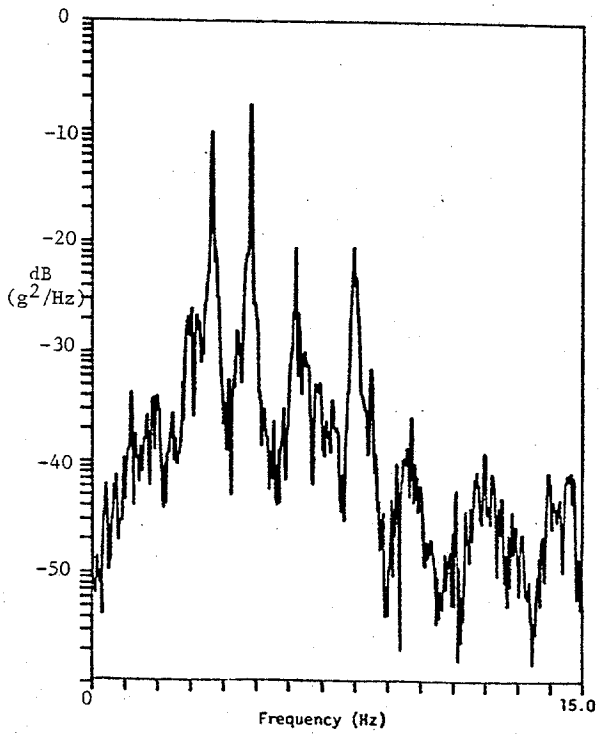

FIG. 11. Spectrum of Simulated In-Line Acceleration

The data presented in the previous section for the non-lock-in cases were analyzed again by using the Case 1 model. The system functions H(W) and $H_1(W)$ were obtained from equations (33) and (30). From the identified system functions H(W) and $H_1(W)$, the spectrums of the residual n(t), the linear and quadratic responses v(t) and y1(t), as well as the simulated in-line response ys(t) were obtained according to,

$$Svv(W)=Sxx(W)|H(W)|^2 \quad (34)$$

$$Sy_1y_1(W)=Sz_1z_1(W)|H_1(W)|^2 \quad (35)$$

$$Sysys(W)=Svv(W)+Sy_1y_1(W) \quad (36)$$

$$Snn(W)=Syy(W)-Sysys(W) \quad (37)$$

A small residual spectrum Snn(W) was obtained which indicated an accurate fit of the Case 1 model to the data. This also meant that higher order nonlinearities were negligible. The spectrum of simulated in-line response Sysys(W) as shown in Figure 11 was in good agreement with in-line response spectrum Syy(W) shown in Figure 5. The spectrum Sysys(W) is almost entirely dominated by the quadratic in-line response. The obtained linear in-line response spectrum Svv(W) was very small and was not shown here. This result is quite different from that of the lock-in case.

Finally, it is interesting to examine the characteristics of the square of the cross-flow response, that is the output $z_1(t)$ from the square-law system in the Case 1 model. Figure 10 shows the spectrum of $z_1(t)$, $Sz_1z_1(W)$, in which the two dominan peaks are located at frequencies exactly equal to that of the in-line response spectrum Syy(W) shown in Figure 5. Figure 12 shows the linear cross-coherence spectrum between $z_1(t)$ and y(t) which demonstrates that these two fluctuating quantities were highly linearly coherent as shown by the high peaks at the two dominant frequencies. This result provided additional evidence of the existence of quadratic correlation between cross-flow and in-line response.

CONCLUSIONS

In conclusion, it should be emphasized that although the results presented in this paper are based on data taken from a single mechanical system, they do suggest that the relationship between cross-flow and in-line response might be best described by a second order nonlinear system for both lock-in and non-lock-in cases. Nonlinear correlations higher than second order were negligible in the nonlinear relationship for both cases. Furthermore, it was indicated in this paper that quadratic transfer functions can be computed by using both time domain and frequency domain multiple regression methods. Knowledge of these transfer functions may be useful in modelling the relationship between cross-flow and in-line response, or equivalently, the lift and drag forces of flow-induced vibration. In addition, for the non-lock-in cases, the square-law system provided a potential way to simplify modelling of the relationship.

In the case of frequency domain analysis, it has been assumed that the non-lock-in cross-flow response is Gaussian. For other applications of quadratic system identification with non-Gaussian input, one can use the time domain multiple regression method to obtain the impulse response kernels. However, the practicality of this method is not clear for a random input case.

ACKNOWLEDGEMENTS

This research represents a segment of a multiyear program at M.I.T. focussed on the understanding of flow-induced vibration. The overall program has had broad federal and industrial support. This particular portion was sponsored by the Technology Assessment and Research Branch of the Minerals Management Service and by the Marine Technology Division of the Naval Research Laboratory.

REFERENCES

1. Bendat, J.S. and Piersol, A.G., "Spectral Analysis of Nonlinear Systems Involving Square-Law Operators," J. of Sound and Vibration, 81(2), 1982.

2. Bendat, J.S. and Piersol, A.G., Random Data: Analysis and Measurement Procedures, John Wiley and Sons, New York, 1971.

3. Brillinger, D.R., Time Series. New York: Holt 1975.

4. Brillinger, D.R. and M. Rosenblatt, "Asymptotic Theory of Estimate of K-th Order Spectra," in Spectral Analysis of Series, B. Harris, Ed. New York: Wiley, 1967.

5. Brillinger, D.R., "Identification of Polynomial Systems by Means of Higher Order Spectra," J. of Sound and Vibration, 12(3), 301-313, 1970.

6. Jenkins, G.M. and Watts, D.G., Spectral Analysis and Its Application, San Francisco, CA: Holden-Day, 1968.

7. Jong, Jen-Yi, "The Quadratic Correlation Between In-Line and Cross-Flow, Vortex-Induced Vibration of Long Flexible Cylinders," MIT Ocean Engineering Department, Ph.D. Dissertation, 1984.

8. Jong, Jen-Yi and Vandiver, J.K., "Response Analysis of the Flow-Induced Vibration of Flexible Cylinders Tested at Castine, Maine in July and August of 1981," MIT Ocean Engineering Department Report, 1983.

9. Kim, Y.C. and Powers, E.J., "Digital Bispectral Analysis and Its Application to Nonlinear Wave Interactions," IEEE Transactions on Plasma Science, Vol. PS7 No. 2, June 1979.

10. Kim, Y.C., Wang, W.F., Powers, E.J., and Roth, J.R., "Extension of the Coherence Function to Quadratic Models," Proceedings of the IEEE, Vol. 67, No. 3, March 1979.

11. Powers, E.J., Choi, D. and Miksad, R.W., "Determination of Nonlinear Drift Force Quadratic Transfer Functions by Digital Cross-Bispectral Analysis," Offshore Technology Conference, Paper No. 4440, 1982.

12. King, R., "A Review of Vortex Shedding Research and Its Application," Ocean Engineering, New England Section, Sept. 26, 1975.

13. Sarpakaya, T., "Vortex Induced Oscillations. A Selective Review," ASME J. of Applied Mechanics, Vol. 46, June 1979, pp. 241.

14. Vandiver, J.K and Griffin, O.M., Measurement of the Vortex Excited Strumming Vibrations of Marine Cable," Proc. of Ocean Structural Dynamics, 1982.

15. Vandiver, J.K., "Natural Frequency, Mode Shape, and Damping Ratios for Cylinders Tested at Castine, Maine in the Summer of 1981," unpublished MIT Ocean Engineering Report.

16. Vandiver, J.K. and Mazal, C.H., "A Field Study of Vortex-Excited Vibrations of Marine Cable," Offshore Technology Conference, OTC Paper No. 2491, Houston, Texas, 1976.

17. Vandiver, J.K., "Drag Coefficients of Long Flexible Cylinders," Offshore Technology Conference, OTC Paper No. 4490, Houston, Texas 1983.

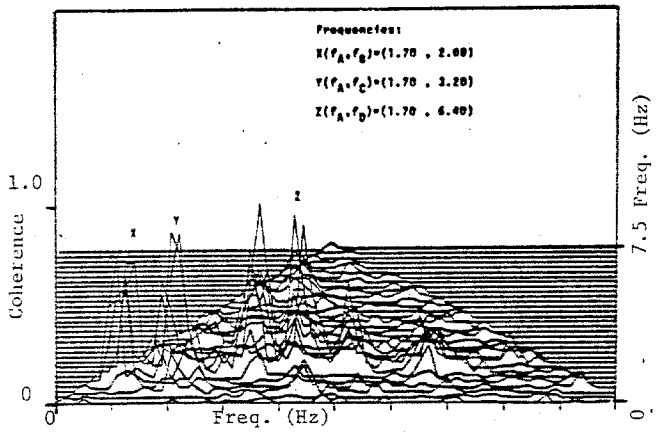

FIG. 7. Cross Bicoherence Between Cross-Flow and In-Line Acceleration

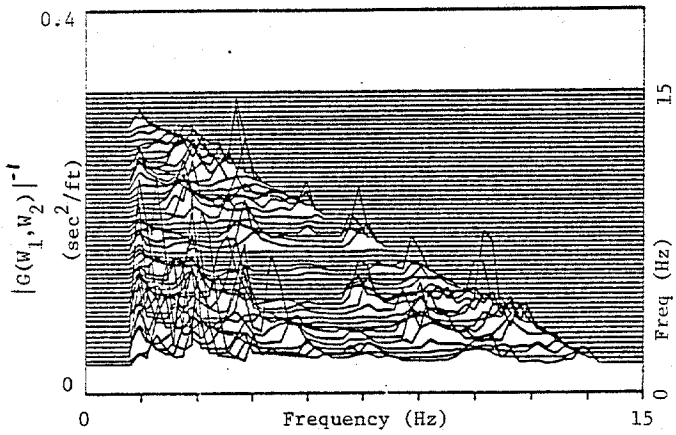

FIG. 8. Quadratic Transfer Function Between Cross-Flow and In-Line Acceleration

Case 1

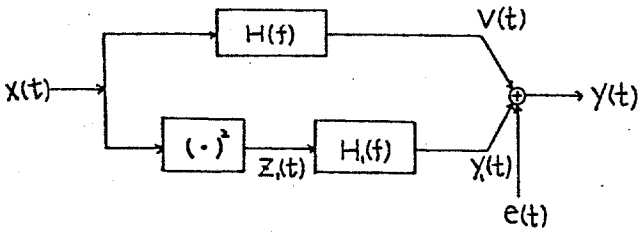

Case 2

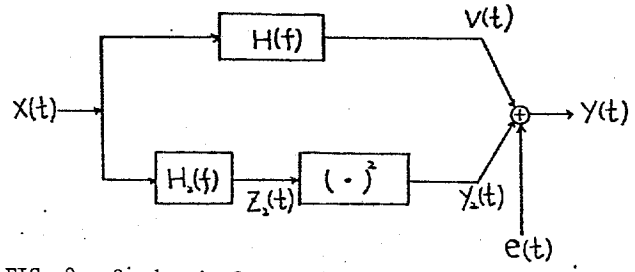

FIG. 9. Quadratic Systems with Square Law Operators

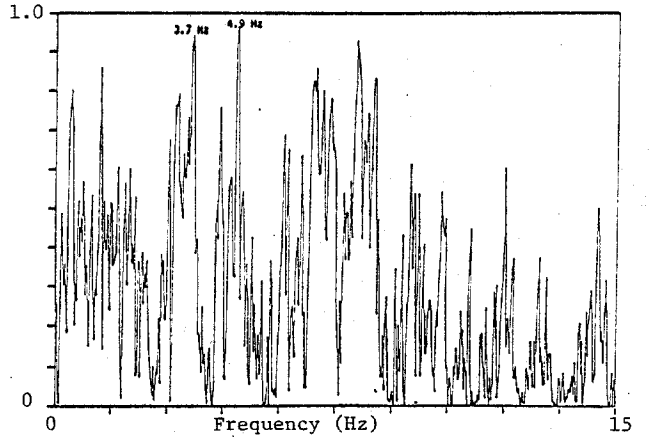

FIG. 12. Linear Coherence Between In-Line Acceleration and the Square of the Cross-Flow Acceleration